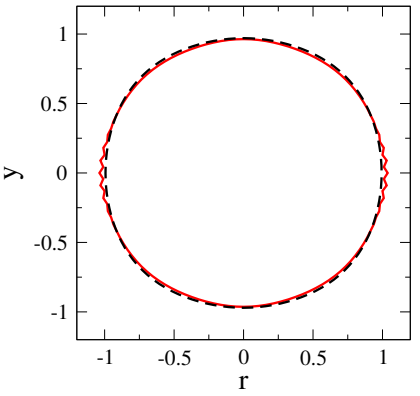

Figure 26: Effect of membrane bending rigidity on the deformation of a capsule with Skalak membrane considering $\sigma_r = 0.1$ and $Ca = 0.45$. Continuous curve represents shape obtained from the boundary integral simulation without considering the effect of bending rigidity and the dashed curve represents the same with $\kappa_b = 0.001$ at $t = 196$.

Appendix B. Supplementary information

B.1. *Importance of incorporating membrane bending*

In the present study, the effect of bending rigidity is clearly demonstrated in fig. 26. Incorporating bending forces eliminate the formation of wiggles. However, it should be mentioned that for deformations with nominal curvatures, it was observed that the results of simulations with and without bending did not have significant differences.

B.2. *Optimization and convergence of the numerical code*

B.2.1. *Number of node points optimization*

Error estimation in the volume inside the capsule (Δv) is conducted for different number elements (number of node points+1) over the half arc length (north pole-south pole) at $\sigma_r = 10$ and $\sigma_r = 0.1$. Analysis has been done at the low deformation, $Ca = 0.25$ at $\sigma_r = 10$ (table 2), as well as in large deformation limits, $Ca = 1$ at $\sigma_r = 10$ (table 3) and $Ca = 0.45$ at $\sigma_r = 0.1$ (table 4). Along with the change in internal volume, the required CPU times per iteration for different number of elements are reported. The computations were done on Intel 5^{th} generation i7 processor. From tables 2 and 4 it can be observed that with the increase of the number of elements the change in internal volume reduces except the results reported in table 3, which is due to the formation of sharp corner at the intermediate large deformation adding error in the measurement of higher order derivatives and thereby in the bending calculation, though the impact is insignificant.

In the current analysis on the deformation of an elastic capsule in DC electric field, the half arc length is divided into 60 elements which keep the change in volume within a considerable limit of $\Delta v < 0.1\%$ for both the cases, $\sigma_r = 0.1$ and 10. Also, as the increase in the number of elements does not improve much in the accuracy of the results but it significantly increases the computational time, we chose to carry out the numerical analysis with 60 elements.

Number of elements	Percent change in volume, Δv (%)	CPU time required per iteration (s)
40	0.142	0.0236
50	0.075	0.0349
60	0.046	0.0532
70	0.031	0.0709
80	0.023	0.0924
90	0.017	0.1159
100	0.014	0.1428

Table 2: Percent change in internal volume of the capsule to reach the steady-state deformation and CPU time required per iteration as a function of number of elements at $Ca = 0.25$ and $\sigma_r = 10$

Number of elements	Percent change in volume, Δv (%)	CPU time required per iteration (s)
40	0.0642	0.0238
50	0.0652	0.0351
60	0.0661	0.0531
70	0.0667	0.0707
80	0.0664	0.0923
90	0.0665	0.1162
100	0.0668	0.1425

Table 3: Percent change in internal volume of the capsule to reach the steady-state deformation and CPU time required per iteration as a function of number of elements at $Ca = 1$ and $\sigma_r = 10$

Number of elements	Percent change in volume, Δv (%)	CPU time required per iteration (s)
40	0.244	0.0248
50	0.132	0.0354
60	0.084	0.0527
70	0.059	0.0692
80	0.036	0.0923
90	0.024	0.1154
100	0.017	0.1426

Table 4: Percent change in internal volume of the capsule to reach the steady-state deformation and CPU time required per iteration as a function of number of elements at $Ca = 0.45$ and $\sigma_r = 0.1$

B.2.2. *Convergence test*

Convergence of the change in internal volume and deformation of a capsule

A numerical computation with 120 elements and $\Delta t = 0.0001$ for the deformation of an elastic capsule at $Ca = 0.45$ and $\sigma_r = 0.1$ is considered as the reference case in which the change in volume is $\Delta v = 0.0006\%$ and degree of deformation is $DD = -0.50313$ at

Number of elements	Percent change in volume, Δv (%)	Degree of deformation, DD
40	0.0202	-0.5034
50	0.0196	-0.5034
60	0.0189	-0.5034
70	0.0184	-0.5034
80	0.0183	-0.5033
90	0.0182	-0.5032
100	0.0182	-0.5032

Table 5: Estimation of change of volume (Δv) and degree of deformation (DD) as function of number of elements at $t = 50$.

Number of elements	Percent change in volume, Δv (%)	Degree of deformation, DD
40	0.0202	-0.4291
50	0.0194	-0.4288
60	0.019	-0.4288
70	0.0186	-0.4288
80	0.0185	-0.4287
90	0.0184	-0.4287
100	0.0183	-0.4287

Table 6: Estimation of change of volume (Δv) and degree of deformation (DD) as function of number of elements at $t = 75$.

$t = 50$ and $\Delta v = 0.0005\%$ and $DD = -0.42868$ at $t = 75$. The change in volume and the degree of deformation of a capsule as a function of number of elements at $Ca = 0.45$ and $\sigma_r = 0.1$ considering $\Delta t = 0.01$ at $t = 50$ and 75 are given in tables 5 and 6, respectively. In both the cases time horizons ($t = 50$ and $t = 75$) are selected when the capsule attains large intermediate deformations. From the analysis, it is justified that the results are fairly converged with respect to change in the number of elements as well as the time step.

Convergence of transmembrane potential of the interface

The transmembrane potential (ϕ_m) of the interface obtained from the numerical calculations with different number of elements (40, 60, 80 and 100) are compared with the obtained ϕ_m for the reference case (number of elements=120 and $\Delta t = 0.0001$) at $t = 50$ (fig. 27a) and $t = 75$ (fig. 27b). In figs. 27a and 27b, very high accuracy in the calculation of ϕ_m is observed for any number of considered elements. The convergence tests for the deformation of a capsule on the change in volume (Δv), degree of deformation (DD) and the transmembrane potential (ϕ_m) of the membrane as a function of number of elements suggest that the selection of 60 elements over the half arc length (north pole-south pole) is justified.

B.3. *Dynamics of capsule with neo-Hookean membrane*

Capsules with a neo-Hookean membrane show very similar intermediate shapes (figs. 28a to 28f) as observed for capsules with a Skalak membrane (figs. 6a to 6f) at $Ca = 0.25$ and $\sigma_r = 0.1$. From the simulated shapes it can be observed that a neo-Hookean capsule passes through the squaring (figs. 28d and 28e) to a steady-state

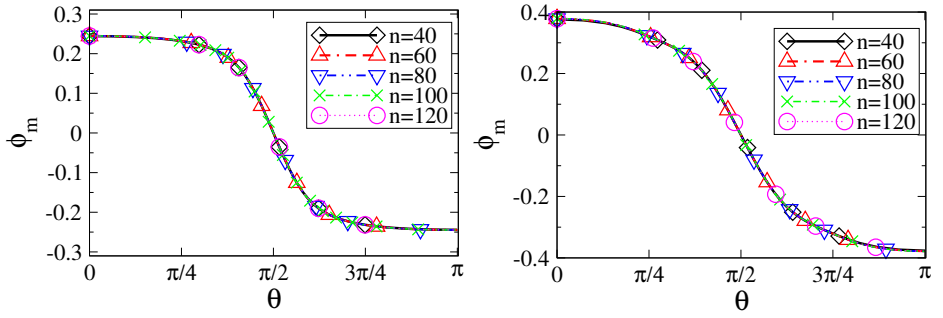

(a) $t = 50$ (b) $t = 75$

Figure 27: Transmembrane potential of the interface ($\theta = 0$ at north pole and $\theta = \pi$ at south pole) for the computation with different numbers of elements.

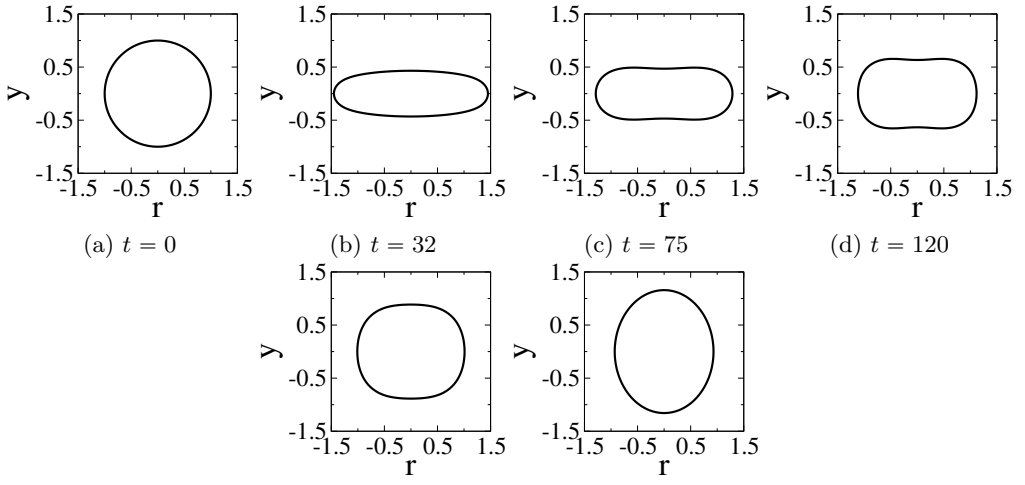

(a) $t = 0$ (b) $t = 32$ (c) $t = 75$ (d) $t = 120$

(e) $t = 175$ (f) $t = \infty$

Figure 28: Shape evolution of a capsule with neo-Hookean membrane at $\sigma_r = 0.1$ for $Ca = 0.25$.

prolate shape (fig. 28f). Just bellow the critical capillary number for breakup ($Ca = 0.29$) a neo-Hookean capsule shows similar intermediate shapes (figs. 29a to 29h) at $\sigma_r = 0.1$ as observed with Skalak capsule (figs. 7a to 7h) at $Ca = 0.45$ and $\sigma_r = 0.1$.

Figure 30 shows shapes during the deformation of neo-Hookean capsule at small capillary number (Ca=0.25) and $\sigma_r = 10$, which are similar to the case of a Skalak capsule at same capillary number (fig. 4) except relatively larger deformation (fig. 20). At high capillary number, $Ca = 0.59$ (fig. 31) a neo-Hookean capsule undergoes very large intermediate deformation (fig. 31c) without forming any sharp corner (observed in the case of a Skalak capsule deformation at $Ca = 2$, fig. 12c) and while relaxing back, unlike a Skalak capsule at large deformation (fig. 12), it shows prolate shapes with $P2(\cos\theta)$ type of perturbation (figs. 31d and 31e).

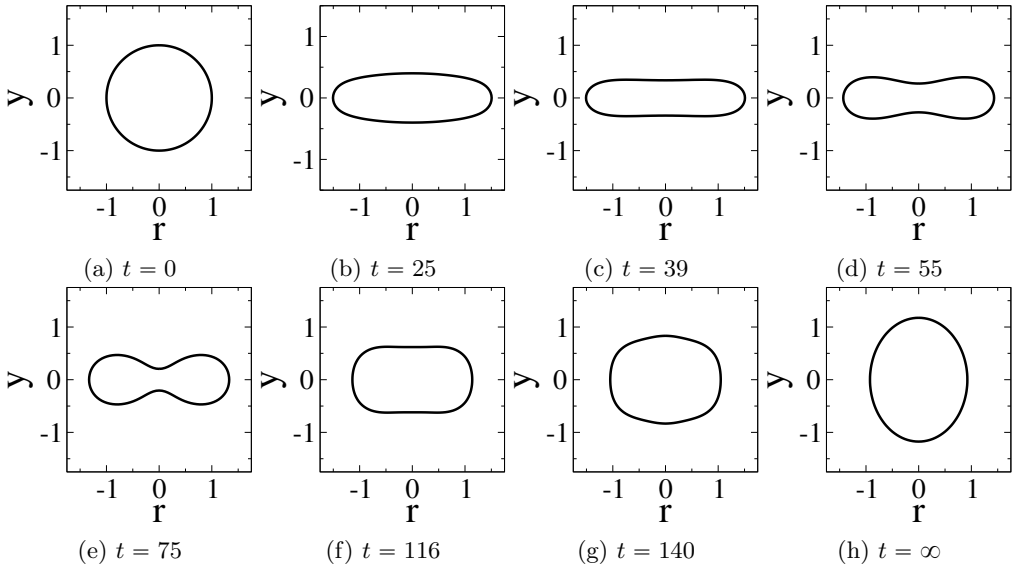

(a) $t = 0$ (b) $t = 25$ (c) $t = 39$ (d) $t = 55$

(e) $t = 75$ (f) $t = 116$ (g) $t = 140$ (h) $t = \infty$

Figure 29: Shape evolution of a capsule with neo-Hookean membrane at $\sigma_r = 0.1$ for $Ca = 0.29$.

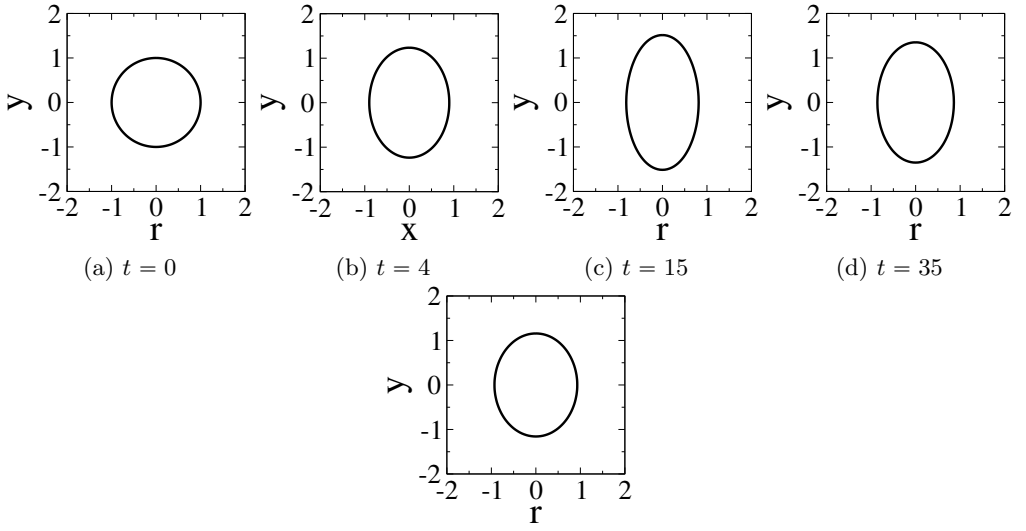

(a) $t = 0$ (b) $t = 4$ (c) $t = 15$ (d) $t = 35$

(e) $t = \infty$

Figure 30: Shape evolution of a capsule with neo-Hookean membrane at $\sigma_r = 10$ for $Ca = 0.25$.

B.4. *Transmembrane potential, normal and tangential electric stresses obtained from AET*

Solutions for the Transmembrane potential, normal and tangential electric stresses obtained from AET are complicated. For the case-specific (considering $G_m = 0$, $C_m = 50$, $\epsilon_r = 1$) expressions for transmembrane potential, normal and tangential electric stresses are given below.

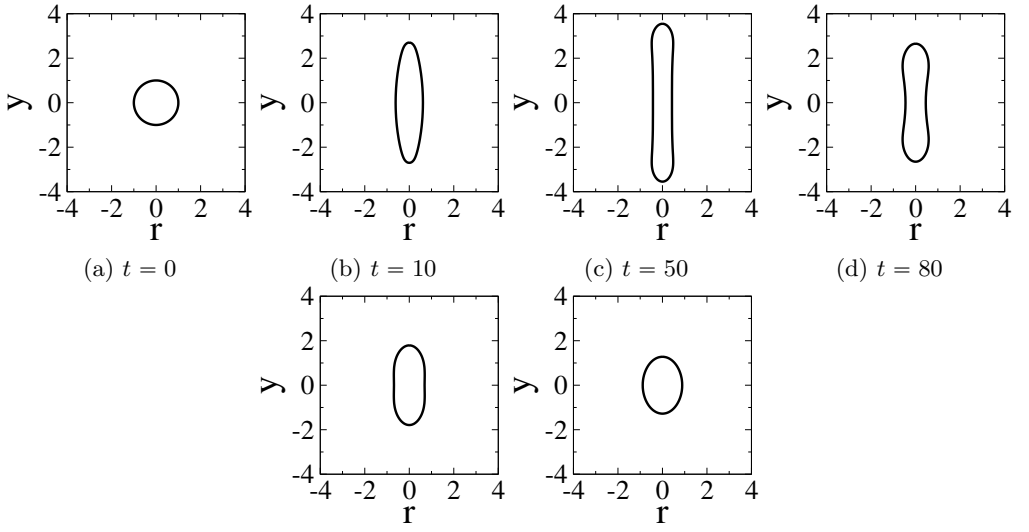

(a) $t = 0$ (b) $t = 10$ (c) $t = 50$ (d) $t = 80$

(e) $t = 95$ (f) $t = \infty$

Figure 31: Shape evolution of a capsule with neo-Hookean membrane at $\sigma_r = 10$ for $Ca = 0.59$.

B.4.1. *For the case of* $\sigma_r = 10$

$$\phi_m = (1.5 - 0.022e^{-4.06t} - 1.478e^{-0.032t})\cos\theta \tag{B 1}$$

$$\tau_n = Ca[(0.799 - 3.833e^{4.027t} + 3.034e^{8.054t})\cos^2\theta + (0.0166 + 1.095e^{4.027t} - 1.106e^{4.059t} - 0.736e^{8.054t} + 1.856e^{8.086t} - 1.125e^{8.119t})\sin^2\theta]e^{-8.12t} \tag{B 2}$$

$$\tau_t = Ca(1.665 - 3.285e^{4.027t} + 2.213e^{4.059t} + 3.12e^{8.054t} - 3.713e^{8.087t})e^{-8.12t}\cos\theta\sin\theta \tag{B 3}$$

B.4.2. *For the case of* $\sigma_r = 0.1$

$$\phi_m = (1.5 - 0.0073e^{-0.703t} - 1.492e{-}0.0018t)\cos\theta \tag{B 4}$$

$$\tau_n = Ca[(0.28 + 0.722e^{0.702t} - 1.002e^{1.403t})\cos^2\theta + (-0.003 - 0.632e^{0.702t} + 0.645e^{0.703t} + 1.01e^{1.403t} + 0.105e^{1.405t} - 1.125e^{1.408t})\sin^2\theta]e^{-1.407t} \tag{B 5}$$

$$\tau_t = Ca(0.549 - 1.083e^{0.702t} - 1.29e^{0.703t} + 2.034e^{1.403t} - 0.21e^{1.405t})e^{-1.407t}\cos\theta\sin\theta \tag{B 6}$$